Supplementary data for

Probing effects of molecular conformation on the electronic and charge transport properties in two- and three-dimensional small molecule hole-transporting materials: A theoretical investigation

Zhu-Zhu Sun,*[a] Shuai Feng,[b] Chuantao Gu,[c] Nian Cheng[a] and Jiangfeng Liu[a]

[a]*Energy-Saving Building Materials Innovative Collaboration Center of Henan Province, Xinyang Normal University, Xinyang 464000, China*

[b]*College of Chemistry and Chemical Engineering, Taishan University, Taian 271021, China*

[c]*College of Materials Science and Engineering, Qingdao University, Qingdao 266071, China*

E-mail: Z.Z.Sun: zhuzhusun@xynu.edu.cn

Table S1 Calculated HOMO energies (in eV) of the investigated HTMs.

HTMs	B3LYP-R[a]	PBE33[b]	CAM-B3LYP[c]	B3LYP[d]
S-1	-5.37	-5.34	-6.00	-4.75
S-2	-5.37	-5.34	-5.98	-4.74
S-3	-5.35	-5.32	-5.98	-4.73
S-4	-5.12	-5.10	-5.78	-4.52
Spiro-OMeTAD	-5.08	-5.07	-5.71	-4.49

[a] The HOMO energies calculated by the semi-rational formula based on the optimized geometries of the B3LYP/6-31g** method.

[b] The HOMO energies calculated by single point energy calculation with the PBE33/6-31g** method based on the optimized geometries of the B3LYP/6-31g** method.

[c] The HOMO energies calculated by the CAM-B3LYP/6-31g** method.

[d] The HOMO energies calculated by the B3LYP/6-31g** method.

Table S2 Calculated orbital energies (in eV) by single point energy calculations with the PBE33/6-31g** method based on the geometries of the B3LYP/6-31g**.

HTMs	E_{H-2}	E_{H-1}	E_H	E_L	E_{L+1}
S-1	-5.38	-5.35	-5.34	-1.20	-1.19
S-2	-5.45	-5.34	-5.34	-1.12	-1.12
S-3	-5.38	-5.36	-5.32	-0.64	-0.57
S-4	-5.36	-5.35	-5.10	-0.96	-0.80
Spiro-OMeTAD	-5.60	-5.10	-5.07	-0.63	-0.62

Table S3 Calculated absorption and emission wavelengths based on the optimized ground-geometries of the B3LYP/6-31g** method.

Method	HTMs	λ_{abs}	ΔE_{EX}	f	λ_{em}	$\Delta\lambda_{st}$
Optimized: B3LYP/6-31g** Excited: BMK/6-31g**	S-1	358	3.46	1.81	415	56
	S-2	366	3.39	2.22	432	66
	S-3	324	3.83	1.36	388	64
	S-4	371	3.34	1.49	437	66
	Spiro-OMeTAD	355	3.49	1.18	404	49
Optimized: B3LYP/6-31g** Excited: MPW1k/6-31g**	S-1	348	3.56	1.93	406	58
	S-2	357	3.47	2.29	425	68
	S-3	316	3.92	1.40	379	63
	S-4	365	3.39	1.49	433	67
	Spiro-OMeTAD	346	3.58	1.21	396	49
Optimized: B3LYP/6-31g** Excited: CAM-B3LYP /6-31g**	S-1	336	3.69	2.11	394	58
	S-2	349	3.55	2.35	417	68
	S-3	311	3.99	1.43	372	61
	S-4	354	3.50	1.60	420	66
	Spiro-OMeTAD	342	3.63	1.21	390	48
Optimized: B3LYP/6-31g** Excited: LC-BLYP/6-31g** (μ=0.33)	S-1	317	3.92	2.28	372	55
	S-2	331	3.75	2.43	397	66
	S-3	298	4.16	1.47	354	56
	S-4	333	3.72	1.70	396	62
	Spiro-OMeTAD	327	3.80	1.24	372	45

Table S4 Calculated absorption and emission wavelengths based on the optimized ground-geometries of the CAM-B3LYP/6-31g** method.

Method	HTMs	λ_{abs}	ΔE_{EX}	f	λ_{em}	$\Delta\lambda_{st}$
Optimized: CAM-B3LYP /6-31g** Excited: BMK/6-31g**	S-1	345	3.59	1.87	415	69
	S-2	357	3.47	2.19	432	74
	S-3	318	3.90	1.32	388	70
	S-4	360	3.45	1.50	437	77
	Spiro-OMeTAD	350	3.54	1.12	404	54
Optimized: CAM-B3LYP /6-31g** Excited: MPW1k/6-31g**	S-1	336	3.69	1.98	406	71
	S-2	349	3.55	2.26	425	76
	S-3	310	3.99	1.37	379	69
	S-4	354	3.50	1.49	433	79
	Spiro-OMeTAD	342	3.63	1.15	396	54
Optimized: CAM-B3LYP /6-31g** Excited: CAM-B3LYP /6-31g**	S-1	325	3.82	2.16	394	69
	S-2	341	3.64	2.32	417	76
	S-3	305	4.06	1.40	372	66
	S-4	343	3.61	1.60	420	76
	Spiro-OMeTAD	337	3.68	1.15	390	53
Optimized: CAM-B3LYP /6-31g** Excited: LC-BLYP/6-31g** (μ=0.33)	S-1	307	4.04	2.30	372	65
	S-2	324	3.83	2.40	397	73
	S-3	293	4.23	1.44	354	61
	S-4	324	3.82	1.70	396	71
	Spiro-OMeTAD	322	3.85	1.18	372	50

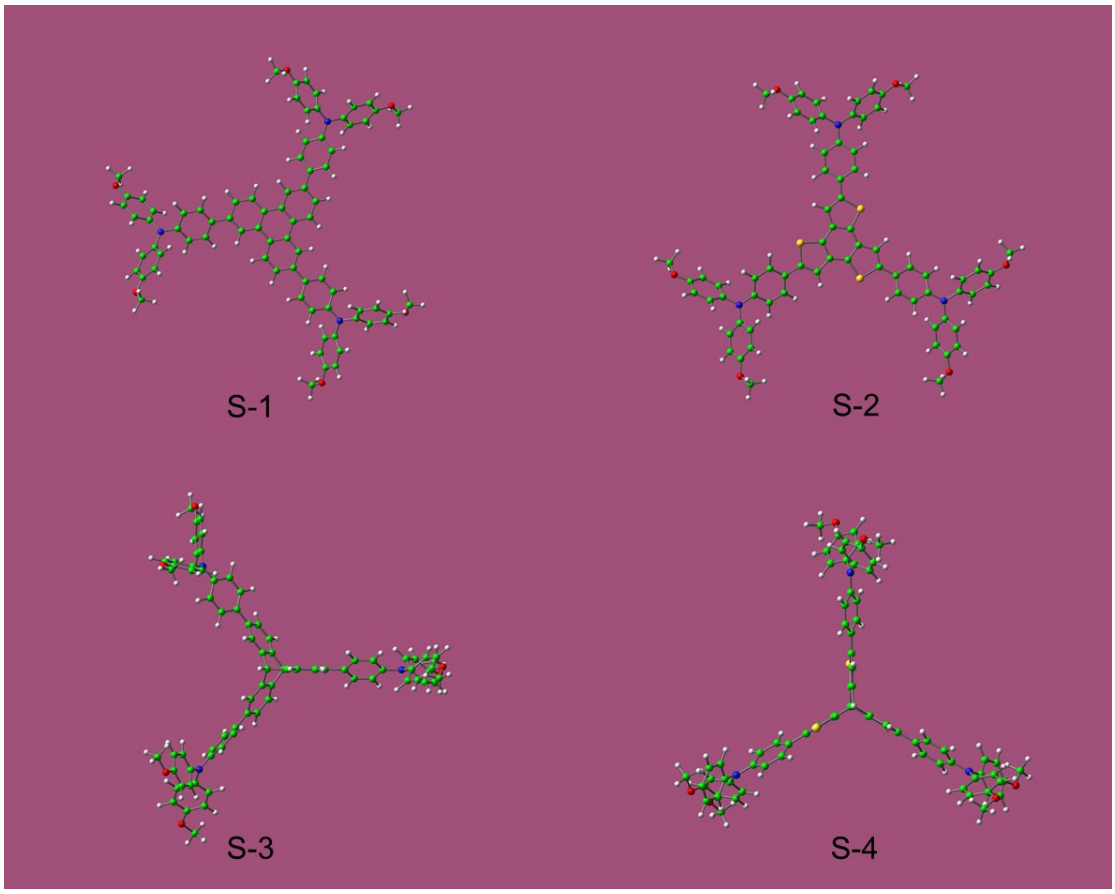

Fig. S1 Optimized molecular geometries of investigated HTMs.

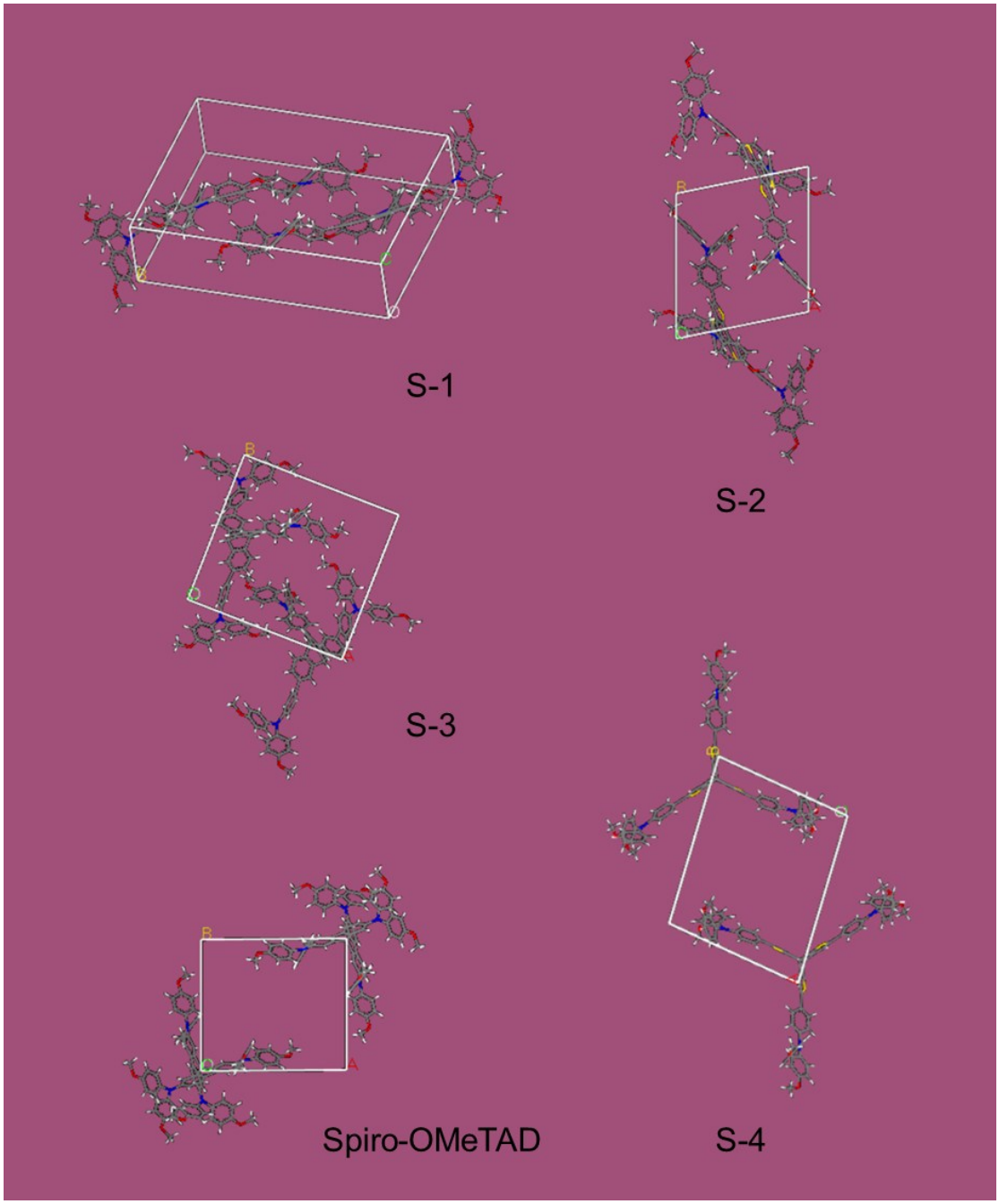

Fig. S2 Predicted crystal structures for the investigated HTMs.

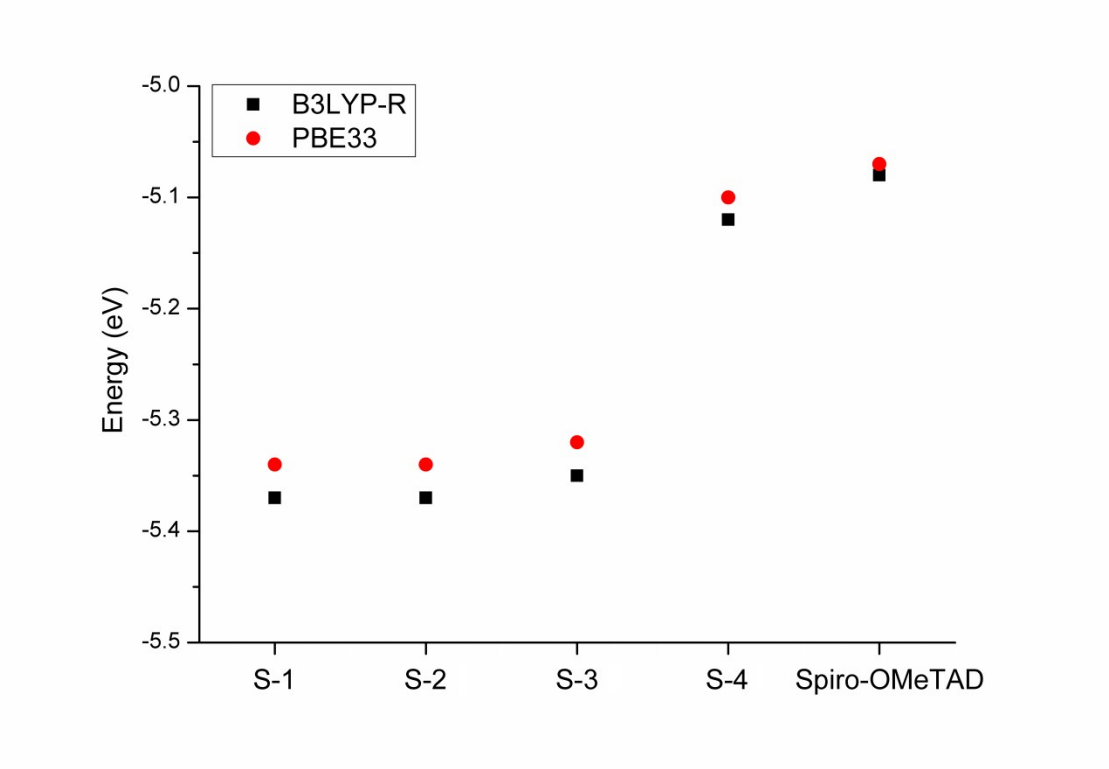

Fig. S3 Calculated HOMO energies of investigated HTMs with the functional B3LYP and PBE33, and the B3LYP-R represents the data revised by semi-rational formula.

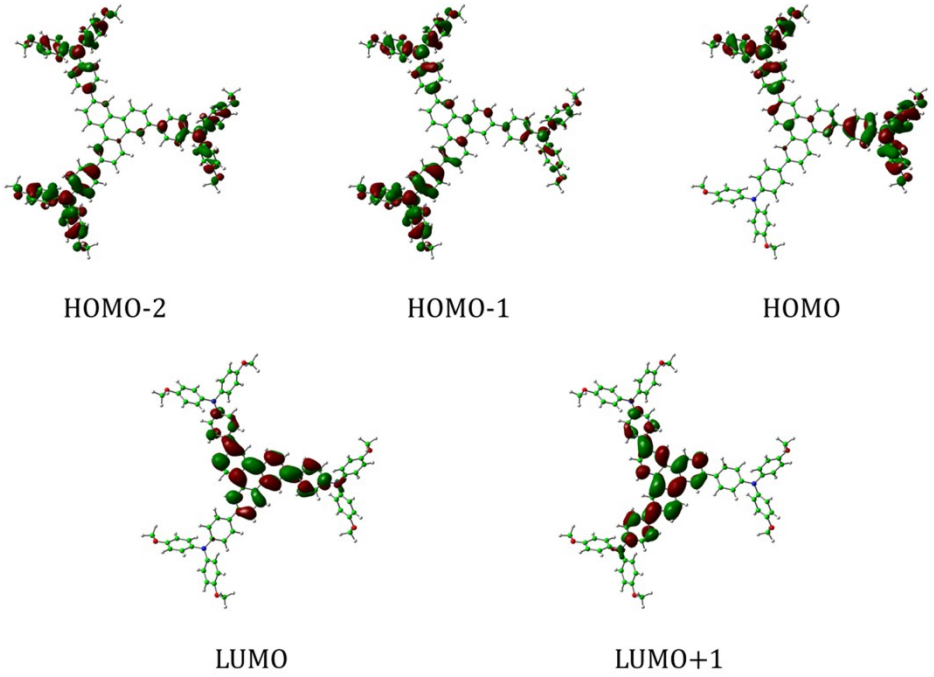

Fig. S4 The orbital distributions of the S-1.

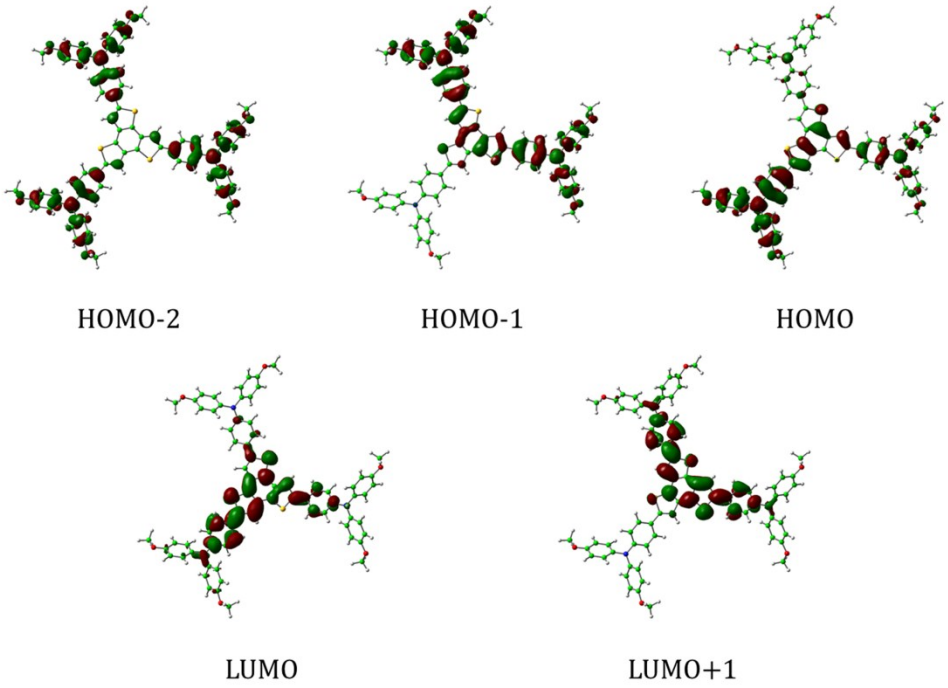

Fig. S5 The orbital distributions of the S-2.

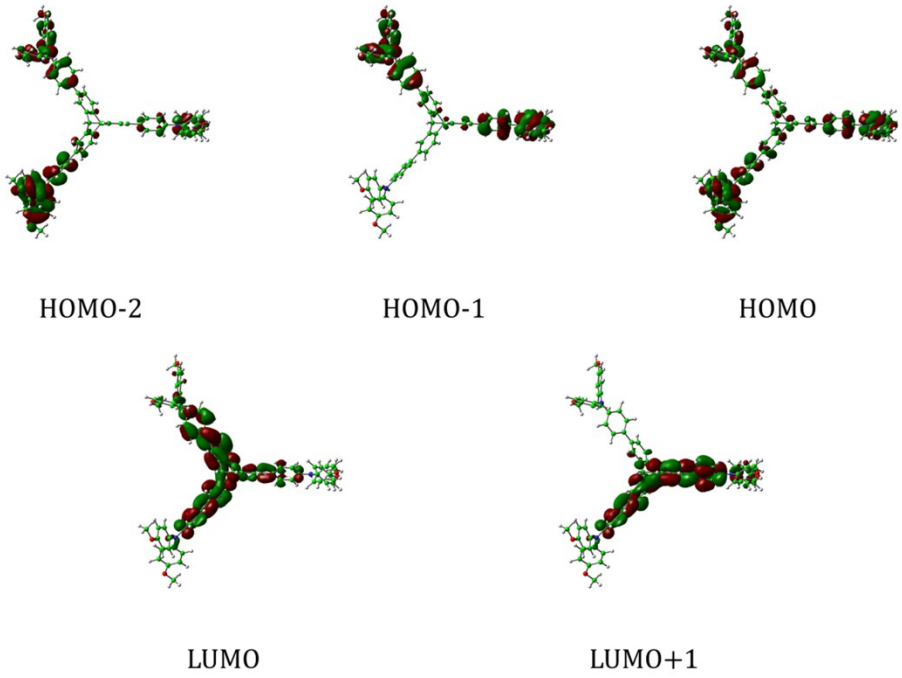

Fig. S6 The orbital distributions of the S-3.

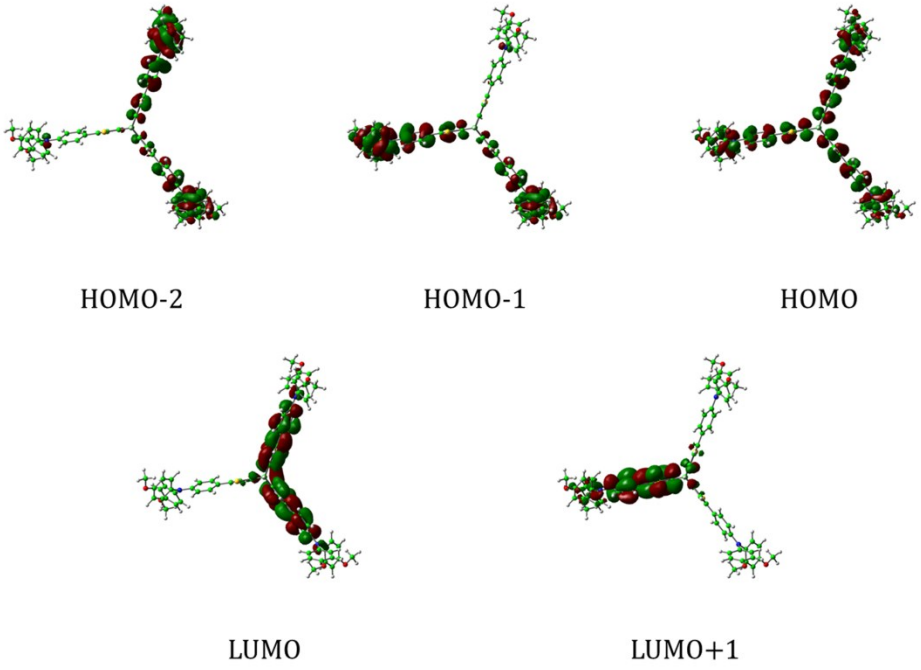

Fig. S7 The orbital distributions of the S-4.

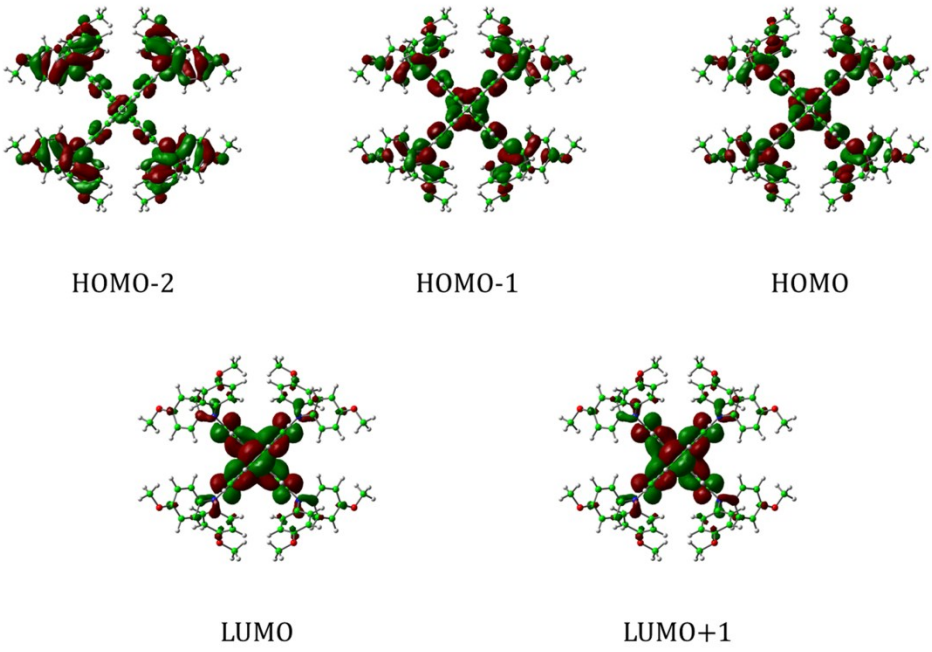

Fig. S8 The orbital distributions of the Spiro-OMeTAD.

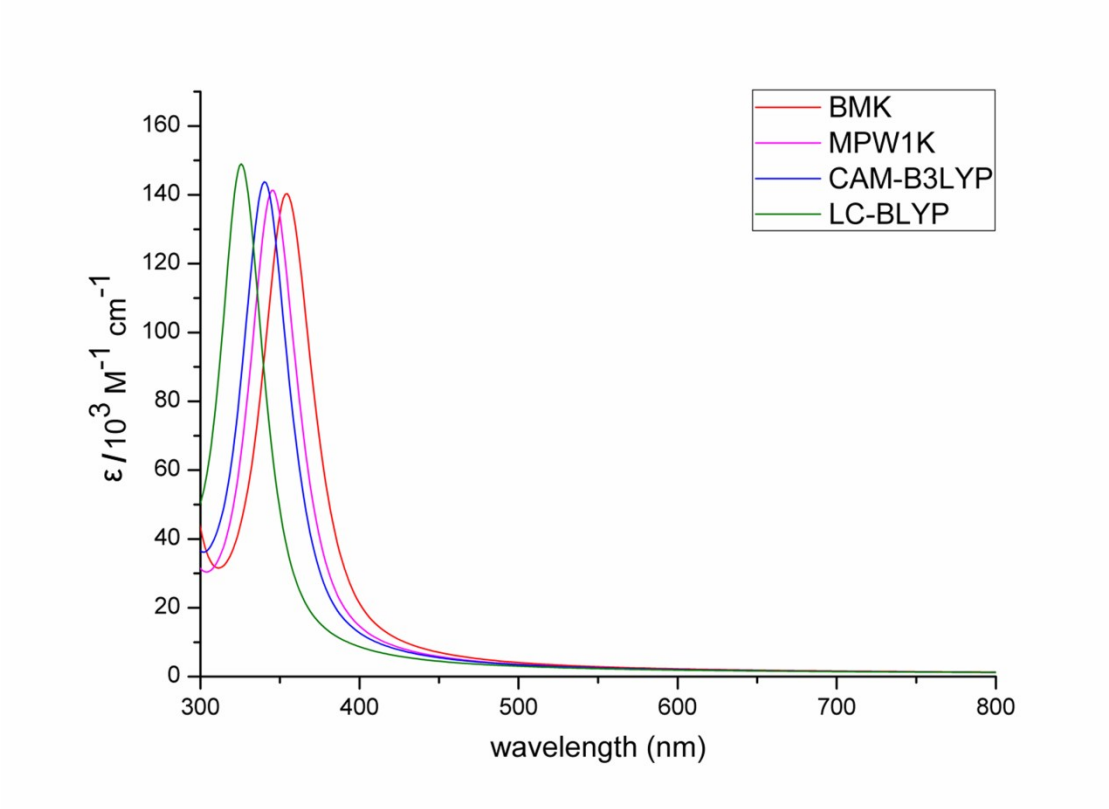

Fig. S9 Calculated absorption spectra of neutral Spiro-OMeTAD with the four typical functionals.